

# Euler equation embedding Double-series Residual neural Network for aero thermal modelling and prediction

<sup>1</sup>Ze Wang, <sup>1</sup>Weiwei Zhang\*, and <sup>1</sup>Shufang Song

<sup>1</sup>*School of Aeronautics, Northwestern Polytechnical University, 710072 Xi'an, China*

**Abstract.** The data-driven aero thermal modeling method provides strong support for the hypersonic aircraft design. In order to improve the accuracy of aero thermal prediction under small training samples and enhance the global geometric generalization ability, this paper proposes Euler equation embedding Double-series Residual neural Network (ED-ResNet). The hypersonic compressible boundary layer theory indicates that the aero thermal loads largely depend on the outer edge information of the boundary layer, and the flow field outside the boundary layer can be regarded as the dominant region of inviscid flow. Based on the above theory, ED-ResNet innovatively embeds the Euler equation into the input front-end of the data-driven model. The performance of the proposed ED-ResNet is validated using hypersonic double-ellipsoid, hypersonic ellipsoid, and blunt cone. The results indicate that with only 4 training samples, ED-ResNet can obtain high-precision aero thermal extrapolation prediction results with an Normalized Root Mean Squared Error (NRMSE) of less than 7% relative to Reynolds-Averaged. Meanwhile, the ED-ResNet can successfully predict aero thermal loads for unknown geometry, with NRMSE less than 13%.

**Keywords:** Aero thermal prediction; data-driven; small-sample modeling; global shape generalization

## 1. Introduction

During the design phase of hypersonic aircraft, it is necessary to accurately predict aero thermal loads[1]. With the rapid development of data science and machine learning, data-driven methods have given strong support for rapid aero thermal prediction[2]. The existing data-driven aero thermal load modeling methods can be mainly divided into three categories, aero thermal feature space dimensionality reduction modeling methods[3,4,5], aero thermal loads pointwise modeling methods[6,7,8], and aero thermal physical information embedding modeling methods[9,10,11,12]. The first two types of data-driven aero thermal load modeling methods have the advantages of simplicity and efficiency, but there are still problems such as large modeling sample size, insufficient geometric generalization ability, and low accuracy upper limit[13]. The most notable feature of the third category of methods is the incorporation of prior physical information or mechanism models into data-driven aerodynamic thermal models, which endows the data-driven models with a certain degree of interpretability, potentially reducing the demand for data samples and enhancing generalization capability.

This research work is based on the ideas of the third category of methods and proposes Euler equation embedding Double-series Residual neural Network, ED-ResNet. Firstly, Euler equation is solved to obtain the inviscid solution on the wall position, and the wall inviscid solution is approximated to the outer edge information of the boundary layer. The wall inviscid solution contains global geometric information of the aircraft, which can improve the global geometric generalization ability of ED-ResNet. Next, consider the numerous physical information contained in the wall inviscid solution. In order to reduce the the number of training samples of ED-ResNet, the physical features of boundary layer outer edge that have the best correlation with aero thermal modeling are provided by combining mechanism model theory knowledge with data-driven model analysis results. Then, D-ResNet is constructed to achieve the prediction of aero thermal loads based on the outer edge features of the boundary layer. Finally, by combining the models of hypersonic double-ellipsoid, hypersonic ellipsoid, and blunt cone, traditional data-driven modeling methods such as POD+Kriging and data-driven modeling methods without embedding Euler equation are compared to verify the small sample modeling ability and global geometric generalization ability of ED-ResNet. The shapes of the supersonic double ellipsoid, supersonic ellipsoid, and blunt cone are shown in Figure 1.

## 2.Method

The specific process of predicting aerothermal loads using ED-ResNet is depicted in Figure 2. ED-ResNet mainly consists of the module for solving Euler equation and the data-driven model D-ResNet, and the bridge between the two is the boundary layer outer edge features.

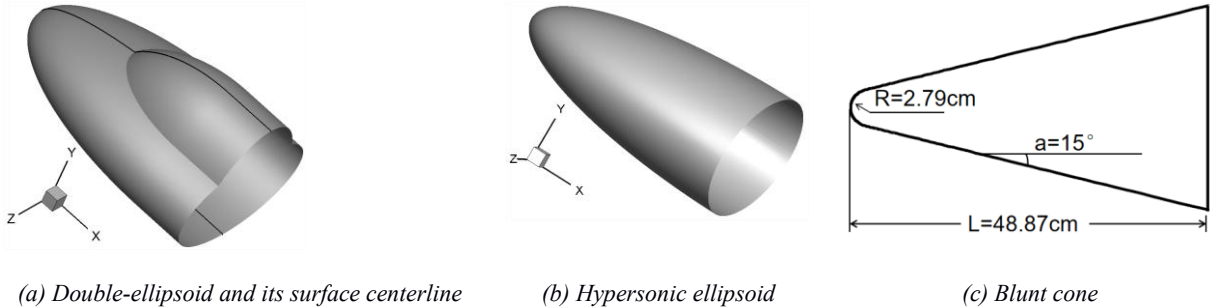


Figure.1 The shapes of the hypersonic double ellipsoid, hypersonic ellipsoid, and blunt cone

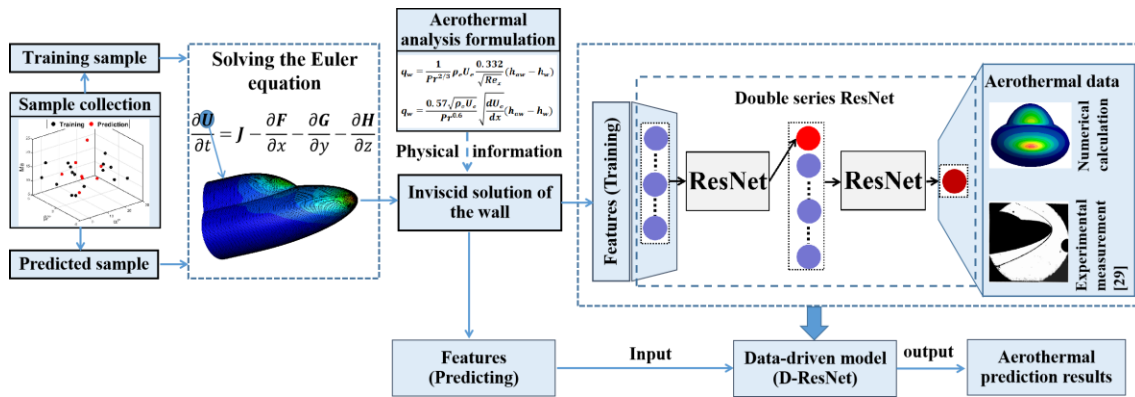


Figure.2 Implementation flowchart of the detailed idea of ED-ResNet

The mechanism equations contain rich physical information that can guide the construction of boundary layer outer edge features. The classic flat plate aerothermal loads calculation Eq. (1) and cylinder stagnation point aerothermal loads calculation Eq. (2) are the most basic equations for calculating aerothermal loads. From these, features that determine the aerothermal distribution are summarized. Using the incoming flow density  $\rho_\infty$ , incoming flow temperature  $T_\infty$ , the 2-norm of the incoming flow velocity  $U_\infty$ , and the reference length of the geometric shape (the distance from the leading edge to the trailing edge)  $L$ , these features are non-dimensionalized to obtain the final boundary layer outer edge features, as shown in Table 1.

$$q = \rho_e U_e \frac{0.332}{\sqrt{Re_s}} (Pr)^{-2/3} (H_{aw} - H_w) \quad (1)$$

$$q = 0.57 Pr^{-0.6} (\rho_e \mu_e)^{0.5} \sqrt{\frac{dU_e}{dx}} (H_{aw} - H_w) \quad (2)$$

The data-driven model D-ResNet is composed of two residual neural networks connected in series, as shown in Figure 3. The inputs of ResNet1 are the distribution of boundary layer outer edge features  $f_i^d = f_i / \max(f_i)$ , and the output is  $q / q_0$ . The inputs of ResNet2 are the boundary layer outer edge features  $f_i$  and the output  $q / q_0$  of ResNet1, and the output of ResNet2 is the non-dimensional aerothermal load  $q / (\rho_\infty U_\infty^3)$ . In D-ResNet, the number of residual blocks for both ResNet1 and ResNet2 is set to 6, the width of dense layers is set to 64.

**Table 1** Features of the outer boundary layer

No.	Physical Interpretation	Feature	No.	Physical Interpretation	Feature
$f_1$	Dimensionless streamline length.	$s_e / L$	$f_2$	Dimensionless flow rate.	$(\rho_e U_e) / (\rho_\infty U_\infty)$
$f_3$	The power of 0.5 of local Reynolds number.	$\sqrt{Re_s}$	$f_4$	Dimensionless temperature difference.	$(T_e - T_w) / T_\infty$
$f_5$	Approximation represents the dimensionless kinetic energy.	$\frac{U_e^2}{U_\infty^2}$	$f_6$	Dimensionless velocity gradients in x direction.	$\frac{d(U_e / U_\infty)}{d(x / L)}$
$f_7$	Dimensionless velocity gradients in y direction.	$\frac{d(U_e / U_\infty)}{d(y / L)}$	$f_8$	Dimensionless velocity gradients in z direction.	$\frac{d(U_e / U_\infty)}{d(z / L)}$

### 3. Results

#### 3.1 Example verification of the modeling and prediction capabilities with small samples and results discussion

OD-ResNet: To verify the importance of the Euler equation embedded in ED-ResNet, the Euler equation is removed from ED-ResNet, and only D-ResNet is used to construct the data-driven model for aero-thermal loads.

E-ResNet: To demonstrate the positive effect of D-ResNet architecture in the ED-ResNet, we replace the D-ResNet part with a single ResNet while retaining the Euler equation embedding.

POD + kriging: A traditional data-driven aero-thermal loads modeling method used for comparative verification of the superiority of ED-ResNet.

Figure 4 shows the NRMSE curve of the aero-thermal loads predicted by ED-ResNet, E-ResNet, OD-ResNet and POD+kriging as a function of the number of training samples, with RANS calculated aero-thermal loads serving as the true values. Under various numbers of training samples, the NRMSE of ED-ResNet is lower than the NRMSE of OD-ResNet, especially in small training samples where the comparison is significant. With just 4 training samples, embedding the Euler equation reduces the NRMSE of data-driven model prediction results by one order of magnitude. This indicates that embedding the Euler equation can significantly reduce NRMSE of the data-driven model prediction results in small sample modeling.

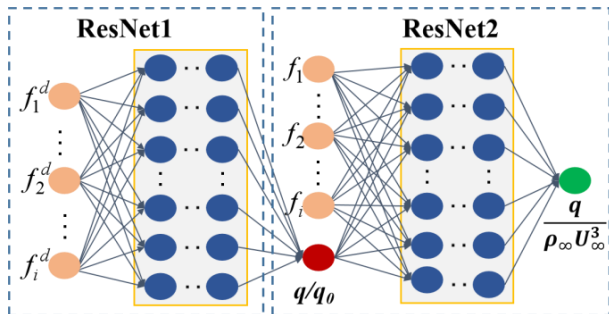


Figure 3 Architecture of D-ResNet

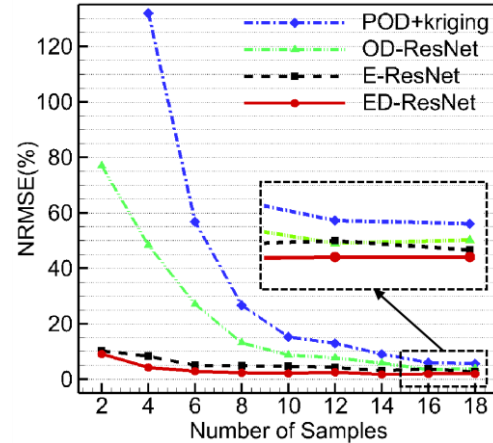


Figure 4 The functional relationship between NRMSE curves and number of training samples for aero-thermal predictions of different models

The incoming flow states of the hypersonic double-ellipsoid training cases and extrapolation test cases, and the NRMSE of the aero-thermal loads predicted by ED-ResNet, are presented in Table 2. The

\*Corresponding Author, Weiwei Zhang [aeroelastic@nwpu.edu.cn](mailto:aeroelastic@nwpu.edu.cn)

results indicate that under the condition of training with a small sample size, the NRMSE of the prediction results for extrapolation test cases using ED-ResNet does not exceed 7%. As shown in Figure 5, a comparison is made between the aerothral results for the extrapolation test case 3 predicted by ED-ResNet and those calculated by RANS; the predicted results align closely with the RANS calculations.

**Table 2** The incoming flow states of the hypersonic double-ellipsoid training cases and extrapolation test cases, and the NRMSE of the aerothral loads predicted by ED-ResNet

Training Cases						Test Cases						
Labels	$Ma_{\infty}$	$\alpha(^{\circ})$	$\beta(^{\circ})$	$T_{\infty}(K)$	$P_{\infty}(Pa)$	Labels	$Ma_{\infty}$	$\alpha(^{\circ})$	$\beta(^{\circ})$	$T_{\infty}(K)$	$P_{\infty}(Pa)$	NRMS E
1	10.5	22.6	4.6	69	121.6	1	12.4	-3.3	-0.3	75	139.1	6.5%
2	18.6	-2.7	-3.6	69	121.6	2	16.7	-0.4	1.6	81	157.0	4.9%
3	11.7	9.7	-0.1	69	121.6	3	13.9	6.1	2.5	63	104.9	4.1%
4	16.0	15.4	2.2	69	121.6	4	15.4	3.8	-4.6	57	89.0	7.0%

### 3.2 Example verification of global geometry generalization and results discussion

To verify the global shape generalization of ED-ResNet, hypersonic ellipsoid cases are used as training samples, while hypersonic double-ellipsoid cases and blunt cone cases are used as test samples. Table 3 shows the incoming flow states of hypersonic ellipsoid training samples, and double-ellipsoid test cases, and the NRMSE of the aerothral loads predicted by ED-ResNet. During the numerical computations of hypersonic ellipsoid and double-ellipsoid,  $T_{\infty}=69K$ ,  $P_{\infty}=121.6Pa$ , and  $T_w=288K$ . Table 4 shows the incoming flow states of blunt cone test cases, and the NRMSE of the aerothral loads predicted by ED-ResNet. It is found from table 3 and table 4 that the NRMSE of aerothral loads predicted by ED-ResNet is less than 13%. Figure 6 and Figure 7 further showed the aerothral contours predicted by ED-ResNet, using hypersonic double-ellipsoid test case 1, blunt cone test case 1 and test case 4 as examples, and compared them with RANS calculation results. It is found that the aerothral contours predicted by ED-ResNet are basically consistent with RANS calculation results.

**Table 3** The incoming flow states of the hypersonic ellipsoid training cases and double-ellipsoid test cases, and the NRMSE of the aerothral loads predicted by ED-ResNet

Hypersonic ellipsoid training cases						Double-ellipsoid test cases						
Labels	$Ma_{\infty}$	$\alpha(^{\circ})$	$\beta(^{\circ})$	Labels	$Ma_{\infty}$	$\alpha(^{\circ})$	$\beta(^{\circ})$	Labels	$Ma_{\infty}$	$\alpha(^{\circ})$	$\beta(^{\circ})$	NRMS E
1	17.4	15.5	1.7	8	10.0	0.0	0.0	1	10.0	0.0	0.0	6.7%
2	19.4	-1.8	-4.1	9	10.0	5.0	0.0	2	8.1	10.9	3.8	8.4%
3	20.5	22.2	3.7	10	10.0	10.1	4.5	3	16.7	-0.4	1.6	7.2%
4	15.2	12.9	2.6	11	10.0	10.0	0.0	4	19.7	13.7	3.5	7.2%
5	13.7	7.6	-0.7	12	10.0	15.0	0.0	5	12.4	-3.3	0.3	6.9%
6	12.3	-0.2	-3.0	13	10.0	20.0	0.0	6	15.4	3.8	4.6	7.0%
7	9.6	20.5	1.0	14	10.0	30.0	0.0	7	13.9	6.1	2.5	5.9%

**Table 4** The incoming flow states of the blunt cone test cases and the NRMSE of the aerothral loads predicted by ED-ResNet

Case Labels	$Ma_{\infty}$	$\alpha(^{\circ})$	$\beta(^{\circ})$	$T_{\infty}/K$	$P_{\infty}/Pa$	NRMSE
1	10.0	0	0	69	121.6	10.0%
2	12.3	-0.2	-3.0	69	121.6	10.7%
3	15.2	12.9	2.6	51	73.9	12.9%
4	13.7	7.6	-0.7	75	139.1	12.3%

Figure 8 compares the ED-ResNet prediction results, Eckert's Reference Temperature Method (ERT) prediction results and RANS calculation results for the aerothral loads on the surface centerline (shown

in Figure 1(a)) of the hypersonic double-ellipsoid test case 5. The results show that when dealing with unknown geometric shapes, the aerothermal load distribution predicted by ED-ResNet still highly agree with the RANS calculation results, compared to the ERT method, the NRMSE still possessing a significant accuracy advantage. The above results demonstrate the excellent global geometric shape generalization capability of the ED-ResNet .

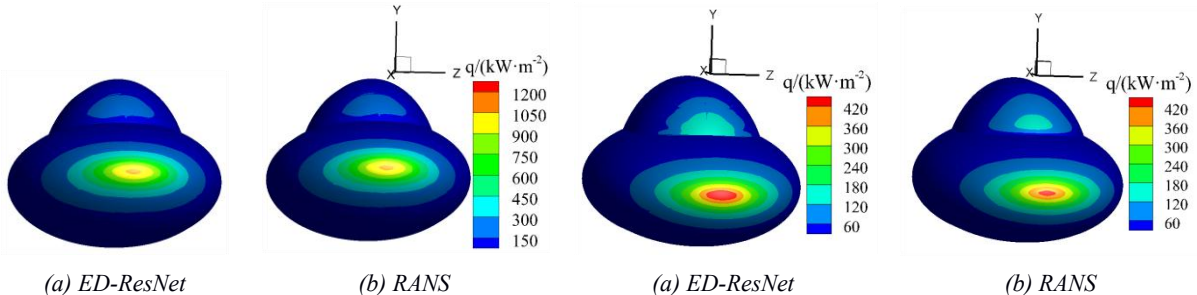


Figure 5 Extrapolation test case 3, a comparison of the aerothermal results predicted by ED-ResNet using 4 training samples and those calculated by RANS.

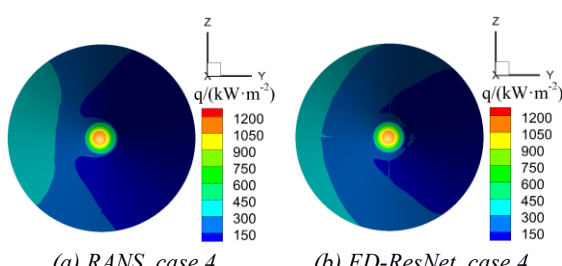


Figure 6 Double-ellipsoid test case 1, a comparison of the aerothermal contours predicted by ED-ResNet using hypersonic ellipsoid training samples and those calculated by RANS

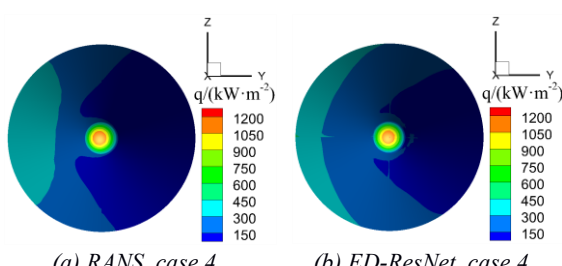


Figure 7 Blunt cone test cases, comparisons of the aerothermal contours predicted by ED-ResNet using hypersonic ellipsoid training samples and those calculated by RANS

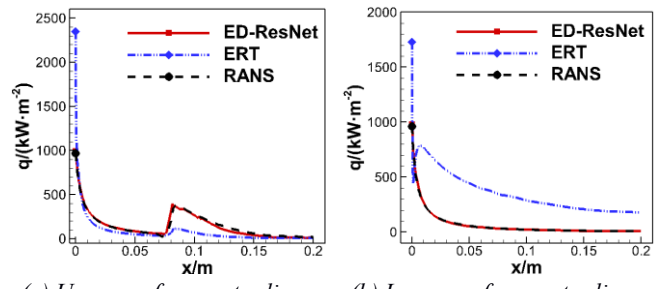


Figure 8 Comparison of ED-ResNet prediction results, ERT prediction results, and RANS calculation results for the aerothermal loads of hypersonic double-ellipsoid test case 5

#### 4. Conclusion

For the aerothermal prediction of hypersonic double-ellipsoid with variable inflow states, ED-ResNet demands only 4 training samples, and the NRMSE of the predicted aerothermal load is less than 7%. Compared with POD+kriging, the NRMSE of aerothermal load predicted by ED-ResNet can be reduced by more than 2 orders of magnitude, which is 1/20 of the NRMSE of aerothermal load predicted by OD-ResNet. The embedding of the Euler equation has brought powerful small sample modeling capability to ED-ResNet. For the aerothermal prediction of variable geometric shapes, ED-ResNet achieves an prediction NRMSE of less than 13%.The embedding of Euler equation enables ED-ResNet to have good generalization ability for geometric shapes, and ED-ResNet can give relatively accurate predictions for aerothermal loads of unknown geometric shapes. In future work, there is potential to build a large model for aerothermal prediction based on the ED-ResNet. However, it is necessary to improve the ED-ResNet to adapt to aerothermal prediction under conditions such as shock-boundary layer interference, transition, and high-temperature chemical reactions, and other disturbances.

#### 5. References

1. McNamara J J and Friedmann P P(2011).*Aeroelastic and aerothermoelastic analysis in hypersonic flow: past, present, and future*.AIAA Journal, **49** (6): 1089-1122.. <https://doi.org/10.2514/1.J050882>

2. Brunton S L, Kutz J N, Manohar K and Aravkin A Y, Klemisch J, Goebel N, Buttrick J, Poskin J, Blom S A, Hogan T and McDonald D(2021). *Data-driven aerospace engineering: reframing the industry with machine learning*. AIAA Journal, **59** (8): 2820-2847. <https://doi.org/10.2514/1.J060131>
3. Liu J, Wang M and Li S (2021). *The rapid data-driven prediction method of coupled fluid-thermal-structure for hypersonic vehicles*. Aerospace, **8** (9). <https://doi.org/10.3390/aerospace8090265>
4. Drouet V, Prevereaud Y, Moschetta J M, Bartoli N, Dubreuil S, Annaloro J(2021). *Reduced order models for heat flux and pressure distributions on space debris afterbodies*. Acta Astronautica, **181**: 446-460. <https://doi.org/10.1016/j.actaastro.2020.12.018>
5. Chen X, Liu L, Long T and Yue Z J(2015). *A reduced order aerothermodynamic modeling framework for hypersonic vehicles based on surrogate and POD*. Chinese Journal of Aeronautics, **28** (5): 1328-1342. <https://doi.org/10.1016/j.cja.2015.06.024>
6. Dreyer E R, Grier B J, Mcnamara J J and Orr B C. *Rapid* (2021). *Steady-State hypersonic aerothermodynamic loads prediction using reduced fidelity models*. Journal of Aircraft, **58** (3): 663-676. <https://doi.org/10.2514/1.C035969>
7. Ding D, Chen H, Ma Z, Zhang B and Liu H (2022). *Heat flux estimation of the cylinder in hypersonic rarefied flow based on neural network surrogate model*. Aip Advances, **12** (8). <https://doi.org/10.1063/5.0108757>
8. Santos M J, Hosder S and West T K (2021). *Multifidelity modeling for efficient aerothermal prediction of deployable entry vehicles*. Journal of Spacecraft and Rockets, **58** (1): 110-123. <https://doi.org/10.2514/1.A34752>
9. Brouwer K R and Mcnamara J J (2020). *Generalized treatment of surface deformation for high-speed computational fluid dynamic surrogates*[J]. AIAA Journal, **58** (1): 329-340. <https://doi.org/10.2514/1.J058470>
10. Zangeneh R(2021). *Data-driven model for improving wall-modeled large-eddy simulation of supersonic turbulent flows with separation*. Physics of Fluids, **33** (12). <https://doi.org/10.1063/5.0072550>
11. Dai G, Zhao W W, Yao S and Chen W F(2023). *Deep-learning strategy based on convolutional neural network for wall heat flux prediction*. AIAA Journal, **61** (11): 4772-4782. <https://doi.org/10.2514/1.J062879>
12. Venegas C V and Huang D (2023). *Physics-infused reduced-order modeling of aerothermal loads for hypersonic aerothemoelastic analysis*. AIAA Journal, **61** (3): 1002-1020. <https://doi.org/10.2514/1.J062214>
13. Wang Z, Wang X, Zhang W and Song S (2024). *ED-ResNet: Euler equation embedding double-series residual neural network for aerothermal modeling*. AIAA Journal. <https://doi.org/10.2514/1.J064012>